Identification of a polymer growth process with an equilibrium multicritical collapse phase transition: The meeting point of swollen, collapsed, and crystalline polymers

Jason Doukas,[1,*] Aleksander L. Owczarek,[1,†] and Thomas Prellberg[2,‡]
[1]*Department of Mathematics and Statistics, The University of Melbourne, Melbourne, Victoria 3010, Australia*
[2]*School of Mathematical Sciences, Queen Mary University of London, Mile End Road, London E1 4NS, United Kingdom*
(Received 13 April 2010; published 1 September 2010)

We have investigated a polymer growth process on the triangular lattice where the configurations produced are self-avoiding trails. We show that the scaling behavior of this process is similar to the analogous process on the square lattice. However, while the square lattice process maps to the collapse transition of the canonical interacting self-avoiding trail (ISAT) model on that lattice, the process on the triangular lattice model does not map to the canonical equilibrium model. On the other hand, we show that the collapse transition of the canonical ISAT model on the triangular lattice behaves in a way reminiscent of the θ point of the interacting self-avoiding walk (ISAW) model, which is the standard model of polymer collapse. This implies an unusual lattice dependency of the ISAT collapse transition in two dimensions. By studying an extended ISAT model, we demonstrate that the growth process maps to a multicritical point in a larger parameter space. In this extended parameter space the collapse phase transition may be either θ-point-like (second order) or first order, and these two are separated by a multicritical point. It is this multicritical point to which the growth process maps. Furthermore, we provide evidence that in addition to the high-temperature gaslike swollen polymer phase (coil) and the low-temperature liquid-drop-like collapse phase (globule) there is also a maximally dense crystal-like phase (crystal) at low temperatures dependent on the parameter values. The multicritical point is the meeting point of these three phases. Our hypothesized phase diagram resolves the mystery of the seemingly differing behaviors of the ISAW and ISAT models in two dimensions as well as the behavior of the trail growth process.

DOI: 10.1103/PhysRevE.82.031103 PACS number(s): 05.50.+q, 05.70.Fh, 61.41.+e

I. INTRODUCTION

Over the past 25 years various lattice models of a single self-interacting polymer chain in (dilute) solution have been analyzed in both two and three dimensions. The fundamental physical phase transition [1] that these models attempt to mimic is that of the collapse of a single polymer in a poor solvent as the temperature is lowered. At high temperatures a polymer is swollen relative to a reference Gaussian state, while at low temperatures the polymer forms a liquid-drop-like globule [1,2]. There is a continuous phase transition expected between these two states, which is referred to as the θ point. One question that arises concerns the robustness of the universality class of the collapse transition. The standard theory [3–5] of the collapse transition is based on the $n \to 0$ limit of the magnetic tricritical $\phi^4 - \phi^6 O(n)$ field theory and related Edwards model with two and three body forces [6,7], which predicts an upper critical dimension of 3 with subtle scaling behavior in that dimension. On the other hand recent studies [8–10] of semiflexible polymers indicate that a third phase appears at low temperatures, namely, a crystal-like phase. The transition between the globular phase and the crystalline phase is first order in three dimensions, while at large enough stiffness the globular phase disappears and a first-order transition occurs directly between the swollen phase and the crystalline polymer. This is essentially in accord with off-lattice studies [11], although the crystalline phase can exist there without the presence of stiffness.

The canonical lattice model of the configurations of a polymer in solution has been the self-avoiding walk (SAW) where a random walk on a lattice is not allowed to visit a lattice site more than once. Self-avoiding walks display the so-called excluded volume effect where they are swollen in size relative to unrestricted random walks of the same length: their size scales with a different characteristic exponent to that of the unrestricted random walk. A common way [1] to model intrapolymer interactions in such a walk is to assign an energy to each nonconsecutive pair of monomers lying on neighboring lattice sites. This is the interacting self-avoiding walk (ISAW) model, which is the standard lattice model of polymer collapse using self-avoiding walks.

On the other hand self-avoiding trails [12], which are lattice random walks that are not allowed to visit a lattice bond more than once, also display the same excluded volume behavior as SAW and physical polymers, with the same scaling exponents. The original motivation for the consideration of trails was to examine the effect of loops or rings on the large-scale behavior of a single polymer. Hence, the answer to that question was considered to be no substantive effect [12]. A self-interacting self-avoiding trail (ISAT) model, where multiply occupied sites are assigned an energy, has also displayed some of the characteristics of the polymer collapse described above [13–16]. However, analyses of both two- and three-dimensional self-interacting trails [14–16] indicate that the collapse transition of the ISAT model is in a different universality class to that of ISAWs in those respective dimensions. There is no clear understanding of why this is the case, if true. It is important to note that work in two

*Present address: Yukawa Institute for Theoretical Physics, Kyoto University, 606-8502, Japan; jasonad@yukawa.kyoto-u.ac.jp
†a.owczarek@ms.unimelb.edu.au
‡t.prellberg@qmul.ac.uk

dimensions has focused on the square lattice model only.

Some of the work [14,15] on the ISAT model has been via a growth process known as "kinetic growth trails" or "smart kinetic trails" that map to one particular temperature of the equilibrium ISAT model on the lattices studied (it is important to note that these lattices are of coordination number 4). It was proposed in [17] that the collapse transition associated with smart kinetic trails is first order. Clear evidence was produced in [17] to demonstrate that there was a first-order transition in three dimensions on the diamond lattice. On the other hand no evidence of this could be found in two dimensions. In fact, on the square lattice recent work [16] verified that the ISAT collapse transition on the square lattice is precisely that given by the growth process and is not first order or like the θ point of ISAW.

Another approach has been to analyze a generalized ensemble (rather than the finite length ensemble) of the model via transfer matrix [18]: this has produced some intriguing results with different values of critical exponents being estimated. It was pointed out in [18] that these results may be compatible with those for the finite length ensemble. This may be an indication though that the point in question is multicritical of some type.

In this paper we study the ISAT model and kinetic growth trails on the *triangular* lattice, importantly a coordination number 6 lattice. We demonstrate that the kinetic growth model does not map to any temperature of the canonical ISAT model but rather to a point (we shall call this the *kinetic growth point*) in the parameter space of a generalized model we call the extended ISAT (eISAT) model. As such we have studied this eISAT model and identify this kinetic growth point as a multicritical collapse point. By studying the eISAT model we build a picture of the collapse transition in the trail model of polymers that includes both the first-order transition suggested in [17] and the ISAW θ point. It may also prove useful in explaining the transfer-matrix results.

Review of previous results

The collapse transition can be characterized via a change in the scaling of the size of the polymer with temperature. There is a strong dimensional dependence on the nature of the transition. We shall focus on the two-dimensional scenario. It is expected that some measure of the size, such as the radius of gyration or the mean squared distance of a monomer from the end points, $R_n^2(T)$, scales at fixed temperature as

$$R_n^2(T) \sim An^{2\nu}, \tag{1.1}$$

where n is the number of monomers in the polymer, with some exponent ν. At high temperatures the polymer is swollen and in two dimensions it is accepted that $\nu=3/4$ [19]. At low temperatures the polymer becomes dense in space, although not space filling, and the exponent is $\nu=1/2$ ($\nu=1/3$ in three dimensions for the comparator state). The collapse phase transition is expected to take place at some temperature T_t. If the transition is second order, the scaling at T_t of the size is intermediate between the high- and low-temperature forms. In the thermodynamic limit there is expected to be a singularity in the free energy, which can be seen in its second derivative (the specific heat). Denoting the (intensive) finite length specific heat *per monomer* by $c_n(T)$, the thermodynamic limit is given by the long-length limit as

$$C(T) = \lim_{n\to\infty} c_n(T). \tag{1.2}$$

One expects that the singular part of the specific heat behaves as

$$C(T) \sim B|T_t - T|^{-\alpha}, \tag{1.3}$$

where $\alpha<1$ for a second-order phase transition. The singular part of the thermodynamic limit internal energy behaves as

$$U(T) \sim B|T_t - T|^{1-\alpha}, \tag{1.4}$$

if the transition is second order, and there is a jump in the internal energy if the transition is first order (an effective value of $\alpha=1$).

Moreover one expects crossover scaling forms [20] to apply around this temperature, so that

$$c_n(T) \sim n^{\alpha\phi}\mathcal{C}([T-T_t]n^{\phi}), \tag{1.5}$$

with $0<\phi<1$ if the transition is second order and

$$c_n(T) \sim n\mathcal{C}([T-T_t]n), \tag{1.6}$$

if the transition is first order. From [20] we point out that the exponents α and ϕ are related via

$$2-\alpha = \frac{1}{\phi}. \tag{1.7}$$

(a) θ-point ISAW collapse. The work of Duplantier and Saleur [21] predicted the standard θ-point behavior in two dimensions, which has been subsequently verified [22]. It is expected that

$$\phi = 3/7 \approx 0.43, \quad \alpha = -1/3. \tag{1.8}$$

Note that this implies that the specific heat does *not* diverge at the transition. However, the third derivative of the free energy with respect to temperature will diverge with exponent $(1+\alpha)\phi=2/7$. We can contrast this with the three-dimensional situation (which is upper critical dimension for this phase transition) where there is a logarithmic divergence in the specific heat. At $T=T_t$ it is expected in two dimensions that $\nu=4/7$, that is,

$$R_n^2(T) \sim An^{8/7}, \tag{1.9}$$

again contrasting with three dimensions where at the θ point a polymer is in a near Gaussian state where $\nu=1/2$.

(b) ISAT collapse on the square lattice. Previous work [16] on the square lattice has shown that there is a collapse transition with a strongly divergent specific heat, and the exponents have been estimated as

$$\phi = 0.84(3), \quad \alpha = 0.81(3). \tag{1.10}$$

At $T=T_t$ it was predicted [14] that

$$R_n^2(T) \sim An(\ln n)^2. \tag{1.11}$$

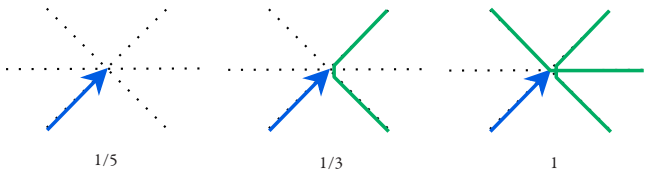

FIG. 1. (Color online) This figure illustrates the growth process on the triangular lattice. Steps are created with different probabilities: the probabilities of the next steps (not shown) are displayed underneath each case. Three general possibilities exist as the trail grows: first is that the trails enter a site that is previously unoccupied—in that case the five choices of next step are chosen at random with equal probability, that is, 1/5; second is that the trail enters a site that has been previously visited once—in that case the three remaining choices of next step are chosen at random with equal probability, that is, 1/3; finally is that the trail enters a site that has been previously visited twice—there is only one choice of continuation and this is made with probability 1.

II. TRAIL GROWTH ON THE TRIANGULAR LATTICE

Consider a stochastic process defined on the triangular lattice as follows: starting at an origin site, a lattice path is built up step by step by choosing between available continuing steps from unoccupied lattice bonds with equal probability. The configuration produced is a *self-avoiding trail* or *trail* for short, where sites may be visited multiple times but bonds of the lattice are either visited once or not at all. If we do not consider the original occupation of the origin as a visit, then each site may be visited up to three times on the triangular lattice. Note that when the process revisits the origin, the growth rule is slightly altered: the process may choose the direction of the first step as one of its options equally with the unoccupied lattice bonds. If it does this, a loop is formed and the growth process terminates. Apart from the initial step, where there are six available steps, the number of available steps is therefore five minus twice the number of previous visits. A picture of these three situations is provided in Fig. 1, along with the probabilities of the *next* step that is added.

In Fig. 2 an example of a configuration produced by the process is illustrated. Apart from the origin, each singly visited site contributes a factor $(\frac{1}{5})$ to the overall probability, while each twice visited site contributes a factor $(\frac{1}{5})(\frac{1}{3})$ and each triply visited site contributes a factor $(\frac{1}{5})(\frac{1}{3})(1)$. This model is the triangular lattice version of the growth model considered previously [14].

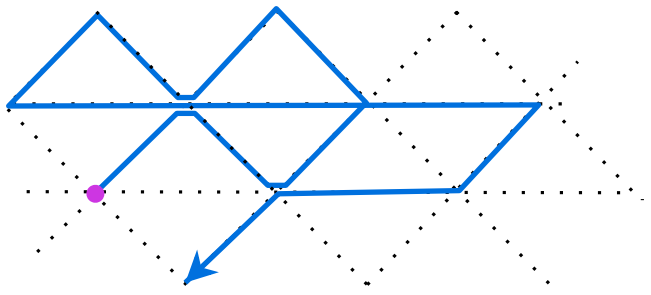

FIG. 2. (Color online) An example of a trail with 13 steps on the triangular lattice. This trail has six singly visited sites, two doubly visited sites, and one triply visited site. Note that the path may cross or touch at a visited site. This trail is produced by the growth process with probability $(\frac{1}{6})(\frac{1}{5})(\frac{1}{5})(\frac{1}{5})(\frac{1}{5})(\frac{1}{3})(\frac{1}{5})(\frac{1}{5})(1)(\frac{1}{3})(\frac{1}{5})(\frac{1}{5})(\frac{1}{3})$—the individual fractional probabilities are the step probabilities in order of creation of the steps.

We will not count the initial occupation of the origin as a visit. If we denote the number of steps of the trail as n, and the numbers of singly, doubly, and triply visited site as m_1, m_2, and m_3, respectively, then these satisfy

$$n = m_1 + 2m_2 + 3m_3. \tag{2.1}$$

The probability of a configuration, φ_n, of n steps is denoted by $p_G(\varphi_n)$, and we have for each n

$$\sum_{\varphi_n} p_G(\varphi_n) = P_n, \tag{2.2}$$

where P_n is the probability that the growth process reaches length n. Let us define the expectation values of the numbers of singly, doubly, and triply visited sites per unit length $e_j(n)$ for the growth process conditioned on the process making it to length n, respectively, as

$$e_j(n) = \frac{\langle m_j \rangle}{n} = \frac{1}{nP_n} \sum_{\varphi_n} p_G(\varphi_n) m_j(\varphi_n), \tag{2.3}$$

and the fluctuations in these as $f_j(n)$ with

$$f_j(n) = \frac{\langle m_j^2 \rangle - \langle m_j \rangle^2}{n}. \tag{2.4}$$

Note that from Eq. (2.1) we have

$$e_1(n) + 2e_2(n) + 3e_3(n) = 1. \tag{2.5}$$

Let us define the asymptotic values of the numbers of doubly and triply visited sites per unit length $e_j(n)$ and their respective fluctuations $f_j(n)$ as

$$E_j = \lim_{n\to\infty} e_j(n), \tag{2.6}$$

$$F_j = \lim_{n\to\infty} f_j(n). \tag{2.7}$$

In the square lattice case [23,24] this stochastic model can be mapped to a specific temperature of an equilibrium model, and moreover [14,16] it was shown that this temperature was a critical point of the equilibrium model. There, the exponents α and ϕ defined in the Introduction can be related to the behavior of e_2 and f_2. Assuming a similar form of critical behavior found in the triangular lattice model we would expect that

$$e_2(n) \sim E_2 - \frac{a_2}{n^{(1-\alpha)\phi}}, \tag{2.8}$$

$$e_3(n) \sim E_3 - \frac{a_3}{n^{(1-\alpha)\phi}}. \tag{2.9}$$

Also,

$$f_2(n) \sim b_2 n^{\alpha\phi} + F_2, \tag{2.10}$$

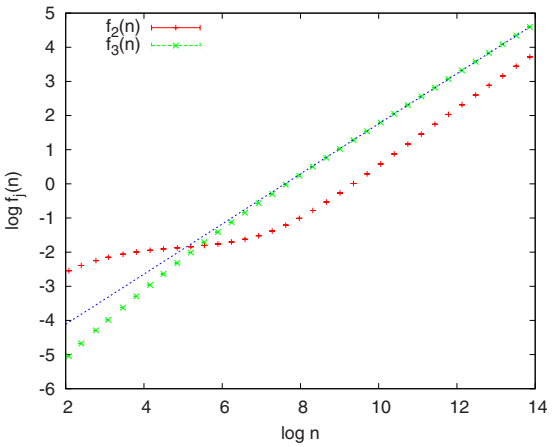

FIG. 3. (Color online) Plot of the fluctuations in the numbers of doubly and triply visited sites $f_2(n)$ and $f_3(n)$ against n. The slope gives us an estimate of $\alpha\phi$.

$$f_3(n) \sim b_3 n^{\alpha\phi} + F_3, \tag{2.11}$$

where either $n^{\alpha\phi}$ or the constant term dominates dependent on whether α is positive or negative.

We have simulated this growth process for lengths up to $n=2^{20}=1\,048\,576$ producing 7 120 000 samples calculating estimates for $e_2(n)$, $e_3(n)$, $f_2(n)$, and $f_3(n)$. In Fig. 3 we plot $f_2(n)$ and $f_3(n)$ against n: we immediately note that both quantities diverge.

Taking the better behaved data for $f_3(n)$, we have estimated

$$\alpha\phi = 0.734(6). \tag{2.12}$$

We can therefore deduce the estimates

$$\alpha = 0.847(3), \quad \phi = 0.867(3). \tag{2.13}$$

Importantly this is consistent with the estimates found in [14] for the growth process on the square lattice where ϕ was estimated to be 0.88(7), subsequently confirmed independently and directly for the equilibrium model in [16] where $\phi=0.84(3)$ was found. Our estimate of $\alpha\phi=0.734(6)$ implies that the exponent involved in the scaling of e_j, namely, $(1-\alpha)\phi$, takes the value of 0.133(4). In Fig. 4 we plot $e_2(n)$ and $e_3(n)$ against $1/n^{0.133}$. We immediately see that the strong corrections to the scaling forms are still apparent even at the long lengths we have simulated. The maximum in $e_2(n)$ at $n \approx 1000$ mirrors the behavior found in $f_2(n)$ in Fig. 3.

In Fig. 4 we have also marked the asymptotic values E_2 and E_3 which can be deduced from the following argument. Consider the case when a trail has formed a large n-step loop which occupies m lattice sites. Any site of this loop could have been the starting point. In order for this site to be visited only once, the loop must have closed at the first return visit, which occurs with a probability of $(\frac{1}{5})$. In order for this site to be visited twice, the loop must have closed at the second return visit, which occurs with a probability of $(1-\frac{1}{5})(\frac{1}{3})$. Finally, for this site to be visited three times, the loop closes at the third return visit, which occurs with a probability of $(1-\frac{1}{5})(1-\frac{1}{3})$. Therefore, we find for large loops the asymptotic values $m_1/m=1/5$, $m_2/m=4/15$, and $m_3/m=8/15$. Using Eq. (2.1), we obtain

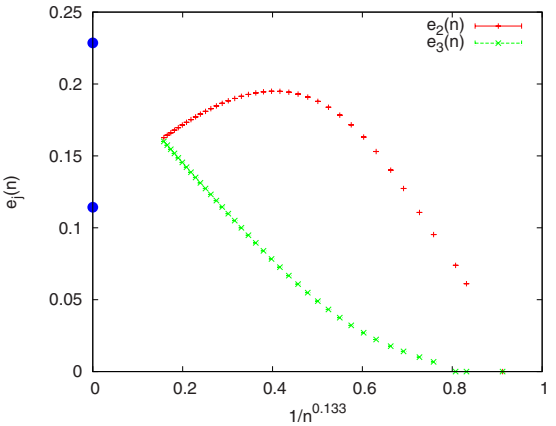

FIG. 4. (Color online) Plot of the average numbers of doubly, $e_2(n)$, and triply, $e_3(n)$, visited sites against $1/n^{0.133}$. Their asymptotic values $E_2=4/35\approx0.114$ and $E_3=8/35\approx0.228$, respectively, are marked as filled circles.

$$e_1(n) \to \frac{3}{35}, \quad e_2(n) \to \frac{4}{35}, \quad e_3(n) \to \frac{8}{35}, \tag{2.14}$$

as $n\to\infty$; whence, we identify $E_2=4/35\approx0.114$ and $E_3=8/35\approx0.228$.

III. CANONICAL ISAT MODEL ON THE TRIANGULAR LATTICE

The canonical model [13] of self-interacting trails (ISAT) on the triangular lattice is defined as follows. Consider all different bond-avoiding paths (open trails and loops) φ_n of length n that can be formed on the triangular lattice with one end fixed at a particular site (the set Ω_n). Associate an energy $-\varepsilon$ with each doubly visited site and an energy -2ε with each triply visited site. For each configuration φ_n count the number $m_2(\varphi_n)$ of doubly visited sites and $m_3(\varphi_n)$ of triply visited sites of the lattice and give that configuration a Boltzmann weight $\omega^{m_2+2m_3}$, where $\omega=\exp(\beta\varepsilon)$. The partition function of the ISAT model is then given by

$$Z_n^{(2)}(\omega) = \sum_{\varphi_n \in \Omega_n} \omega^{m_2(\varphi_n)+2m_3(\varphi_n)}. \tag{3.1}$$

We use the superscript (2) to denote the canonical model. The choice of this notation will become clear in the next section. The average of any quantity Q over the ensemble set Ω_n of allowed paths of length n is given generically by

$$\langle Q \rangle_n(\omega) = \frac{\sum_{\varphi_n \in \Omega_n} Q(\varphi_n)\omega^{m_2(\varphi_n)+2m_3(\varphi_n)}}{Z_n^{(2)}(\omega)}. \tag{3.2}$$

The reduced free energy $\kappa_n^{(2)}(\omega)$ per step is given by

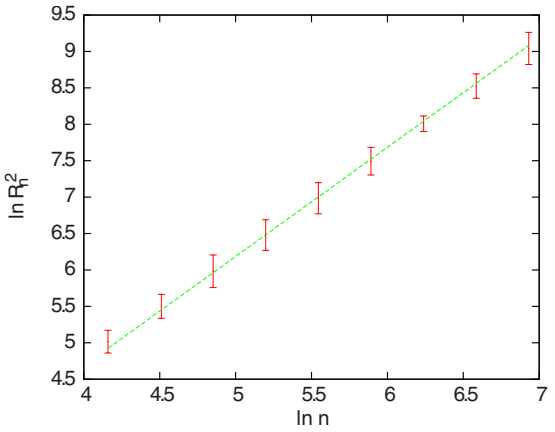

FIG. 5. (Color online) A plot of $\ln R_n^2$ against $\ln n$ at $(\omega_2,\omega_3)=(1.5,2.25)$ in the swollen phase showing a slope of $2\nu=3/2$.

$$\kappa_n^{(2)}(\omega) = -\frac{1}{n}\ln Z_n^{(2)}(\omega), \tag{3.3}$$

and the internal energy $u_n^{(2)}(\omega)$ and specific heat $c_n^{(2)}(\omega)$ can be found as the first and second derivatives of the reduced free energy with respect to β. We will also require the third derivative $t_n^{(2)}(\omega)$. However, these can all be found from the expected values of moments of m_2 and m_3. The internal energy (setting $\varepsilon=1$) is given by

$$u_n^{(2)}(\omega) = \frac{\langle m_2 + 2m_3\rangle}{n}, \tag{3.4}$$

and the (reduced) specific heat is given by

$$c_n^{(2)}(\omega) = \frac{\langle (m_2+2m_3)^2\rangle - \langle (m_2+2m_3)\rangle^2}{n}. \tag{3.5}$$

We have simulated the canonical ISAT model using FLATPERM [25] for lengths up to 1024, generating 1.6×10^7 samples at that length. First we consider a high-temperature point at $\omega=1.5$ and show that the scaling of the size of the trail is in accord with $\nu=3/4$ and the standard swollen phase expectations: in Fig. 5 we display a plot of $\ln R_n^2$ against $\ln n$.

By considering the specific heat we find a weak phase transition in contrast to that found on the square lattice. There is little sign that the specific heat diverges: in Fig. 6 the value of the maximum of the specific heat is plotted against $\ln n$.

We recall that the θ-point transition of ISAW has this nondivergent specific heat behavior, and so we have considered the third derivative of the free energy with respect to β, $t_n^{(2)}(\omega)$, which would diverge slowly for the θ point. The third derivative of the free energy is the first derivative of the specific heat. In Fig. 7 we display the absolute value of the two peaks of the third free-energy derivative. The third derivative has two peaks: one positive and one negative in value. They show a weak divergence: we have extracted local exponents in both cases, which would be given by $(1+\alpha)\phi$, where this is a critical point. We find the values of 0.23(6) and 0.35(6): this is consistent with the ISAW θ point,

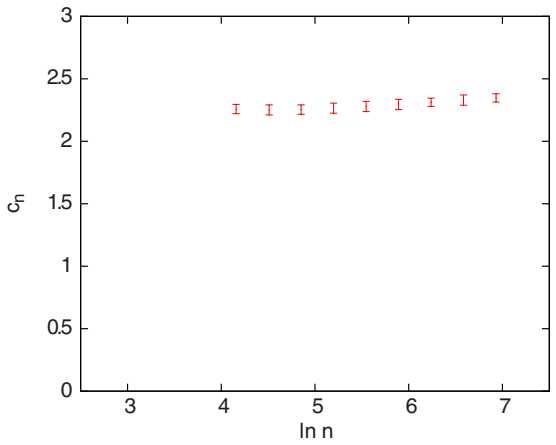

FIG. 6. (Color online) Plot of the value of the maximum of the specific heat $c_n=\max_\omega c_n^{(2)}$ against $\ln n$. This suggests that the specific heat does not diverge as the polymer length is increased.

where $(1+\alpha)\phi=2/7\approx0.28$. While there are clearly very strong corrections to scaling still in the data, no divergence is found in the specific heat and a weak one in the third derivative. Therefore, it is tempting to conjecture that the canonical ISAT model on the triangular lattice has a collapse transition

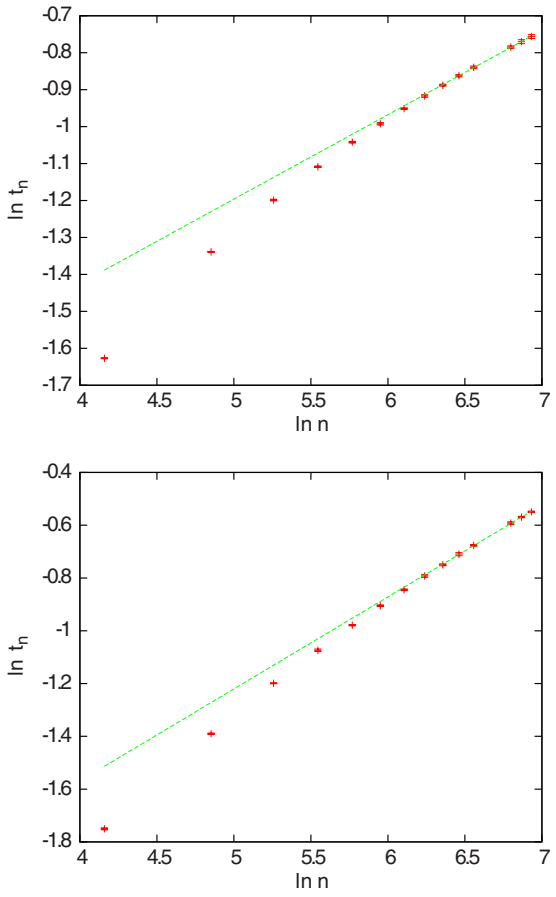

FIG. 7. (Color online) Plot of the height of the peaks of $t_n^{(2)}(\omega)$, the third derivative of the free energy with respect to temperature against n. The third derivative has two peaks: one positive and one negative in value. The top figure shows $t_n=\max_\omega t_n^{(2)}$ and the bottom figure shows $t_n=\min_\omega t_n^{(2)}$.

that lies in the θ-point universality class, rather than in square lattice ISAT collapse universality class.

IV. EXTENDED ISAT MODEL ON THE TRIANGULAR LATTICE

A. Model

The extended model of self-interacting trails (eISAT) on the triangular lattice is defined as follows. Consider all different bond-avoiding paths φ_n (open trails and loops) of length n that can be formed on the triangular lattice with one end fixed at a particular site (the set Ω_n). Associate an energy $-\varepsilon_2$ with each doubly visited site and a different energy $-\varepsilon_3$ with each triply visited site. For each configuration φ_n count the number $m_2(\varphi_n)$ of doubly visited sites and $m_3(\varphi_n)$ of triply visited sites of the lattice and give that configuration a Boltzmann weight $\omega_2^{m_2}\omega_3^{m_3}$, where $\omega_j=\exp(\beta\varepsilon_j)$. The partition function of the eISAT model is then given by

$$Z_n(\omega_2,\omega_3)=\sum_{\varphi_n\in\Omega_n}\omega_2^{m_2(\varphi_n)}\omega_3^{m_3(\varphi_n)}. \tag{4.1}$$

The probability of a configuration φ_n in the equilibrium model is

$$p_E(\varphi_n;\omega_2,\omega_3)=\omega_2^{m_2(\varphi_n)}\omega_3^{m_3(\varphi_n)}/Z_n(\omega_2,\omega_3). \tag{4.2}$$

The average of any quantity Q over the ensemble set of allowed paths Ω_n of length n is given generically by

$$\langle Q\rangle(n;\omega_2,\omega_3)=\sum_{\varphi_n\in\Omega_n}Q(\varphi_n)p_E(\varphi_n). \tag{4.3}$$

Let us define the expectation values of the number of j-fold visited sites per unit length u_j for the equilibrium model as

$$u_j(n;\omega_2,\omega_3)=\frac{\langle m_j\rangle}{n}=\frac{1}{n}\sum_{\varphi(n)}p_E(\varphi(n))m_j(\varphi(n)), \tag{4.4}$$

and the fluctuations in these as c_j with

$$c_j(n;\omega_2,\omega_3)=\frac{\langle m_j^2\rangle-\langle m_j\rangle^2}{n}. \tag{4.5}$$

Note that from Eq. (2.1), which holds for trail configuration regardless of how they are generated, we have

$$u_1+2u_2+3u_3=1. \tag{4.6}$$

The canonical ISAT model is then given by the restriction

$$\omega_2=\omega,\quad \omega_3=\omega^2. \tag{4.7}$$

By fixing the ratio of the energies $\varepsilon_3/\varepsilon_2=k$ we have the generalization

$$\omega_2=\omega,\quad \omega_3=\omega^k, \tag{4.8}$$

which gives a family parametrized by k of generalized one-parameter ISAT models. This gives the partition function of our fixed k versions of the eISAT model as

$$Z_n^{(k)}(\omega)=\sum_{\varphi_n\in\Omega_n}\omega^{m_2(\varphi_n)+km_3(\varphi_n)}. \tag{4.9}$$

Setting $\varepsilon_2=1$ the internal energy is

$$u_n^{(k)}(\omega)=\frac{\langle(m_2+km_3)\rangle}{n}, \tag{4.10}$$

and the (reduced) specific heat is

$$c_n^{(k)}(\omega)=\frac{\langle(m_2+km_3)^2\rangle-\langle(m_2+km_3)\rangle^2}{n}. \tag{4.11}$$

The canonical ISAT model has $k=2$.

We have simulated the general eISAT with a two-parameter FLATPERM algorithm [25] up to length of 128, generating $8.8.6\times10^7$ samples at that length. We have also simulated various specific subcases for fixed values of k via one-parameter FLATPERM algorithm typically up to length of 1024, generating in each case roughly 10^7 samples at that length.

B. Mapping of the growth process to the equilibrium model

The growth process on the square lattice has been mapped [23,24] to a specific Boltzmann weight of the equilibrium model by considering loops. The probability distribution $p_G(\varphi_n)$ of the growth process on the triangular lattice can be rewritten in terms of $m_j(\varphi_n)$ as

$$\begin{aligned}p_G(\varphi_n)&=\frac{1}{6}\left(\frac{1}{5}\right)^{m_1(\varphi_n)-1}\left(\frac{1}{15}\right)^{m_2(\varphi_n)}\left(\frac{1}{15}\right)^{m_3(\varphi_n)}\\&=\frac{1}{6}\left(\frac{1}{5}\right)^{n-1}\left(\frac{5}{3}\right)^{m_2(\varphi_n)}\left(\frac{25}{3}\right)^{m_3(\varphi_n)},\end{aligned} \tag{4.12}$$

using the relationship given in Eq. (2.1). We then notice that by setting $\omega_2=5/3$ and $\omega_3=25/3$ the equilibrium model has probability distribution

$$p_E\left(\varphi_n;\frac{5}{3},\frac{25}{3}\right)=\frac{1}{Z_n\left(\frac{5}{3},\frac{25}{3}\right)}\left(\frac{5}{3}\right)^{m_2(\varphi_n)}\left(\frac{25}{3}\right)^{m_3(\varphi_n)}, \tag{4.13}$$

and so we can deduce

$$p_G(\varphi_n)\propto p_E\left(\varphi_n;\frac{5}{3},\frac{25}{3}\right). \tag{4.14}$$

Note that the normalization is different though since the sum over all walks of fixed length n gives the probability of walks being still open in the case of the growth process, and unity in the case of the equilibrium model.

We now consider the probability of producing configurations in the growth process conditioned on the process having continued to length n, that is, we consider

$$\hat{p}_G(\varphi_n)=\frac{p_G(\varphi_n)}{P_n}, \tag{4.15}$$

which implies that

$$\sum_{\varphi_n\in\Omega_n}\hat{p}_G(\varphi_n)=1. \tag{4.16}$$

Hence, we have

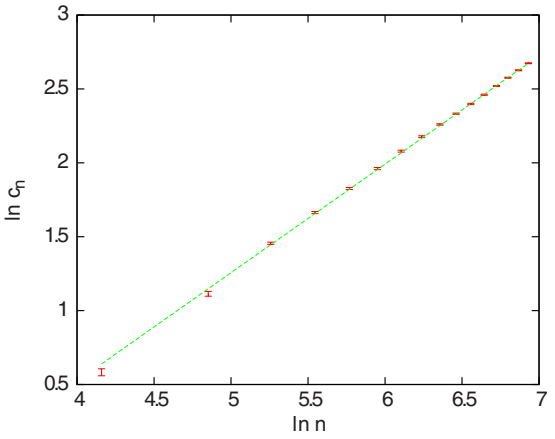

FIG. 8. (Color online) Plot of the logarithm of $c_n=\max_\omega c_n^{(k_G)}$, the value of the maximum of the specific heat, against $\ln n$. The straight line has a slope of 0.734.

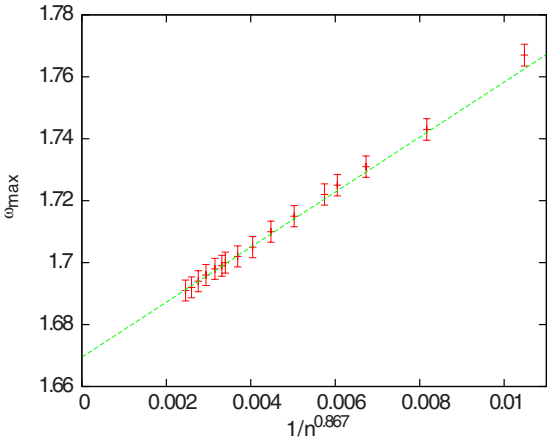

FIG. 9. (Color online) Plot of the location ω_{max} of the peak of the specific heat against $1/n^{0.867}$.

$$\hat{p}_G(\varphi_n) = p_E\left(\varphi_n; \frac{5}{3}, \frac{25}{3}\right), \tag{4.17}$$

noting that this implies that

$$Z_n\left(\frac{5}{3}, \frac{25}{3}\right) = 65^{n-1} P_n. \tag{4.18}$$

In any case, when we simulate the growth process we are effectively simulating the equilibrium eISAT model at the point $(\omega_2, \omega_3)=(5/3, 25/3)$. We immediately have

$$e_j(n) = u_j\left(n; \frac{5}{3}, \frac{25}{3}\right), \quad f_j(n) = c_j\left(n; \frac{5}{3}, \frac{25}{3}\right). \tag{4.19}$$

Using the definition of the one-parameter family of models via Eq. (4.8), the growth process is equivalent to $\omega=5/3$ in the model where

$$k = k_G \equiv \frac{\ln(25/3)}{\ln(5/3)} \approx 4.15. \tag{4.20}$$

Importantly, this is not the value of k for the canonical ISAT model (with $k=2$) on the triangular lattice that has been studied via exact enumeration [13].

C. $k=k_G$ eISAT model

As described in Sec. II we have simulated the growth process and found divergent fluctuations in the numbers of doubly and triply visited sites—a sign of critical behavior. Now that we have mapped the growth process onto a specific temperature of the $k=k_G$ eISAT model, we can verify that this point is indeed the collapse transition point. We have simulated the $k=k_G$ model up to length of 1024 using a one-parameter FLATPERM algorithm. We find a divergent specific heat with a single pronounced peak near $\omega=5/3$. We begin by finding the location and size of the peak of the specific heat of the model. In Fig. 8 we plot the logarithm of the peak height of the specific heat against $\ln n$ along with a line corresponding to the exponent value $\alpha\phi=0.734$, which was obtained from the growth process. Moreover, using the finite length estimate of $\phi=0.867$ obtained from the growth process to extrapolate the location of the transition (see Fig. 9), we find an estimate of $\omega_t=1.669(4)$: this is consistent with the growth process point at $\omega=1.66\dot{6}$ being the transition point.

While the exponent estimates clearly discount a first-order transition, given that there was a question about the first-order nature of the ISAT model on the square lattice at the kinetic growth point, we now show how the distribution of the numbers $m=m_2+k_G m_3$ changes as the temperature is moved through the transition point: this is displayed in Fig. 10. There is no sign of first-order behavior in the distributions.

To complete our numerical analysis we provide a scaling plot around the transition of the specific heat using the exponent values from the growth process. This is found in Fig. 11 and it shows an excellent fit to the crossover scaling form [20]

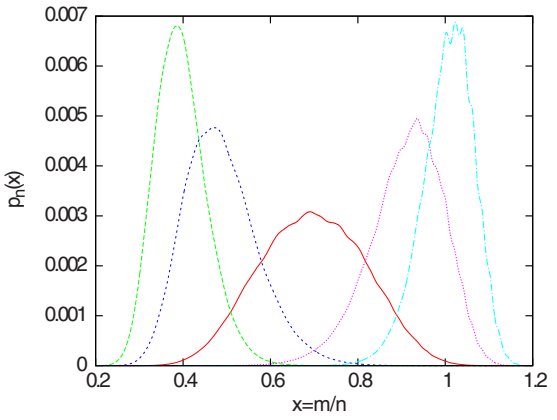

FIG. 10. (Color online) Plot of the distribution $p_n(m/n)$, where $m=m_2+k_G m_3$, at temperatures near and at the temperature at which the specific heat attains its maximum for length $n=1024$. The specific heat attains its maximum at $\omega=\omega_{max}=1.69$ and the distribution is plotted for this value and at $\omega=1.63$, 1.66, 1.72, and 1.54: the plots move from left to right as ω is increased.

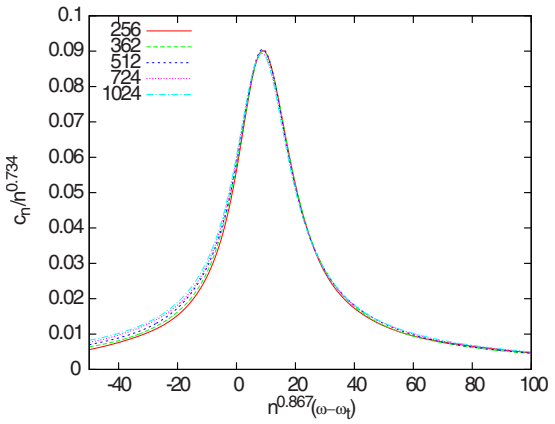

FIG. 11. (Color online) Scaling plot of the specific heat around the transition temperature, using the exponents from the growth process.

$$c_n \sim n^{\alpha\phi}\mathcal{C}([\omega-\omega_t]n^{\phi}). \tag{4.21}$$

Our data at length of 1024 there fully confirm that the kinetic growth point is the location of a phase transition and, moreover, that this transition is critical in nature. The exponent values indicate that the ISAT model on the square lattice and the $k=k_G$ eISAT model on the triangular lattice are in the same universality class. This is in contrast to the observation above that the canonical ISAT models on the two lattices are *not* in the same universality class. This inexorably leads us to the conclusion that the universality class of the phase transition of the eISAT model on the triangular lattice depends on the value of k.

D. $k=0$ eISAT model

To explore this k dependency more we now examine the $k=0$ eISAT model. When $k=0$ only doubly visited sites are given a Boltzmann weight, so that

$$Z_n^{(0)}(\omega) = \sum_{\varphi_n\in\Omega_n} \omega^{m_2(\varphi_n)}. \tag{4.22}$$

The internal energy is

$$u_n^{(0)}(\omega) = \frac{\langle m_2\rangle}{n}, \tag{4.23}$$

and the specific heat is

$$c_n^{(0)}(\omega) = \frac{\langle m_2^2\rangle - \langle m_2\rangle^2}{n}. \tag{4.24}$$

In Fig. 12 the value of the maximum of the specific heat over all ω is plotted against $\ln n$. In stark contrast to the behavior of the $k=k_G$ model but in common with the $k=2$ canonical model, the specific heat does not seem to diverge as the length is increased. In common with the approach we took for the $k=2$ model, we have also examined the third derivative of the free energy. In Fig. 13 we see that the absolute maximum of this quantity is weakly divergent with an exponent of 0.23(6). This compares well to the θ-point value of $2/7\approx 0.28$, especially given the relatively short lengths of the simulations. It is tempting then to conjecture that $k=0$ and $k=2$ models have collapse transitions in the same universality class and that this class is the θ point.

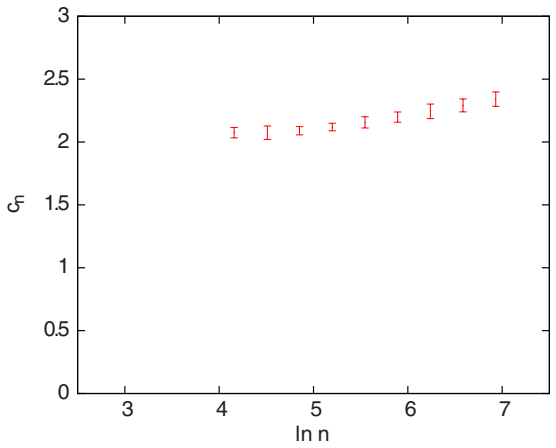

FIG. 12. (Color online) Plot of the value of the maximum of the specific heat $c_n=\max_\omega c_n^{(0)}$ against $\ln n$. This suggests that the specific heat does not diverge as the polymer length is increased, as is the case in the canonical model ($k=2$).

E. Triple model ("$k=\infty$")

Next we consider a model where only triply visited sites are weighted—essentially a $k=\infty$ eISAT—that is, the partition function is given by

$$Z_n^{(triple)}(\omega) = \sum_{\varphi_n\in\Omega_n} \omega^{m_3(\varphi_n)}. \tag{4.25}$$

The internal energy is

$$u_n^{(triple)}(\omega) = \frac{\langle m_3\rangle}{n}, \tag{4.26}$$

and the specific heat is

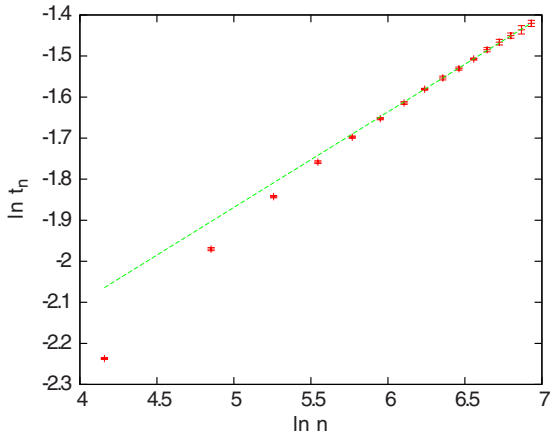

FIG. 13. (Color online) Plot of the height of one of the peaks of $t_n^{(0)}(\omega)$, the third derivative of the free energy with respect to temperature against n. The third derivative has two peaks: one positive and one negative in value. The figure shows $t_n=\min_\omega t_n^{(0)}$ which is the larger in absolute value and the one seemingly less affected by corrections to scaling.

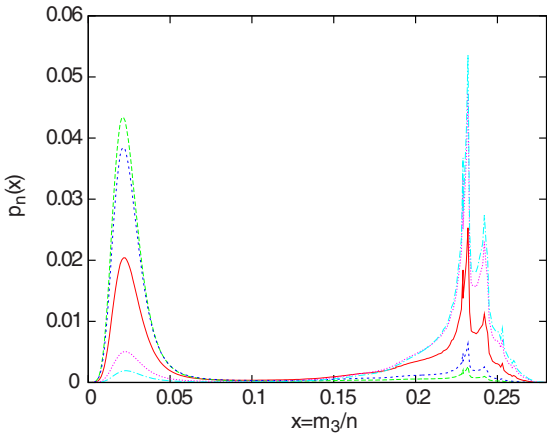

FIG. 14. (Color online) Plot of the distribution $p_n(m_3/n)$ of triply visited sites for the *triple* model at temperatures near and at the temperature at which the specific heat attains its maximum for length $n=1024$. The specific heat attains its maximum at $\omega=\omega_{\max}=7.41$ and the distribution is plotted for this value and at $\omega=7.31$, 7.34, 7.48, and 7.52: the plots move from left to right as ω is increased.

$$c_n^{(triple)}(\omega) = \frac{\langle m_3^2\rangle - \langle m_3\rangle^2}{n}. \tag{4.27}$$

Note that only in the triple model $\omega=\omega_3$, while for the finite k models we denote $\omega=\omega_2$.

As a function of ω we find evidence for a very strong phase transition. In fact when we considered the scaling of the peaks of the specific heat they scale faster than linearly (linearly is the maximum theoretical asymptotic behavior). Since linear behavior would indicate a first-order phase transition we considered the distribution of triply visited sites at temperatures around that which gives rise to the peak of the specific heat: this is plotted in Fig. 14. The distribution displays an unambiguous double peaked form, which is a clear sign of a first-order phase transition. Note the sharpness of the transition in temperature and how the distribution moves from being peaked around low values of triply visited sites just below the transition temperature to being peaked around large values just above the transition temperature. This is a classic first-order behavior. To get an idea of where the transition takes place in the thermodynamic limit we have extrapolated the transition location in Fig. 15. We estimate a thermodynamic limit value of $\omega_t(triple)=6.96(6)$.

We now see that when triply visited sites are weighted the transition is clearly first order, while when doubly visited sites are the only ones given additional weight the transition is a weak second-order transition, like the θ point. In between, the growth model displays intermediate behavior.

F. General eISAT model

To understand whether the first-order nature of the collapse transition persists when doubly weighted sites are given some weight, we have examined the $k=6$ model. Once again the divergence of the specific heat is very strong, and plotting the distribution of triply visited sites (see Fig. 16) the classic doubly peaked form is once again apparent. It

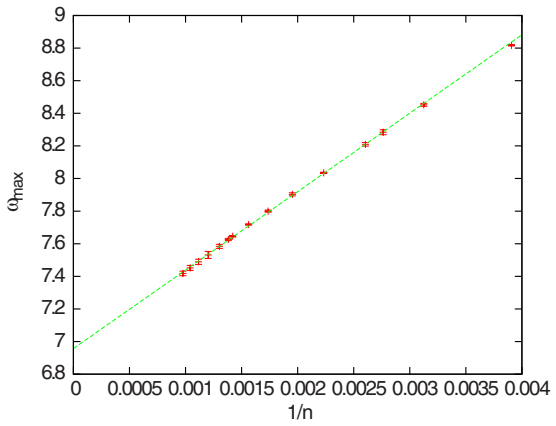

FIG. 15. (Color online) Plot of the location $\omega_{\max}$ of the peak of the specific heat against $1/n$ for the triple model.

seems that the first-order nature persists for large finite values of k. Given the evidence available, the simplest scenario that presents itself is the following: for values of $k>k_G$ the eISAT model on the triangular lattice displays a first-order phase transition, while for $k<k_G$ the model displays a weak second-order transition presumably in the universality class of the ISAW θ point. Separating these two behaviors is the $k=k_G$ model, where the transition is second order but with a divergent specific heat in the universality class of square lattice ISAT. This implies that the growth process point is a multicritical point that is the meeting of a line of first-order transitions to a line of critical ones.

The question then arises as to the nature of the low-temperature phase for different k's. In Fig. 17 we give a density plot of the largest eigenvalue of the matrix of second derivatives of the free energy with respect to the two variables ω_2 and ω_3 at length $n=128$: this allows us to search for any other possible transitions. Intriguingly this plot shows evidence for transitions at large ω_2 and ω_3. This would seem to indicate a collapse-collapse phase transition with two dif-

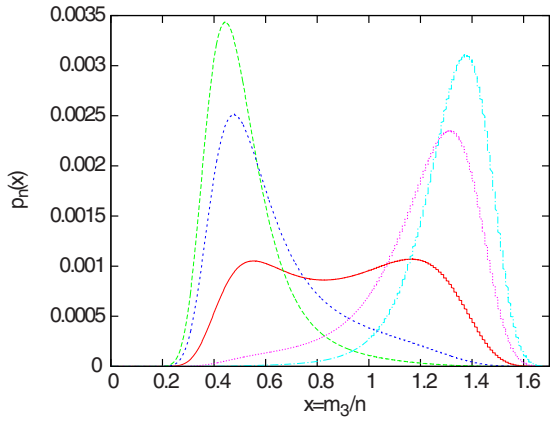

FIG. 16. (Color online) Plot of the distribution $p_n(m_3/n)$ of triply visited sites for the $k=6$ model at temperatures near and at the temperature at which the specific heat attains its maximum for length $n=1024$. The specific heat attains its maximum at $\omega=\omega_{\max}=1.419$ and the distribution is plotted for this value and at $\omega=1.410$, 1.414, 1.425, and 1.430: the plots move from left to right as ω is increased.

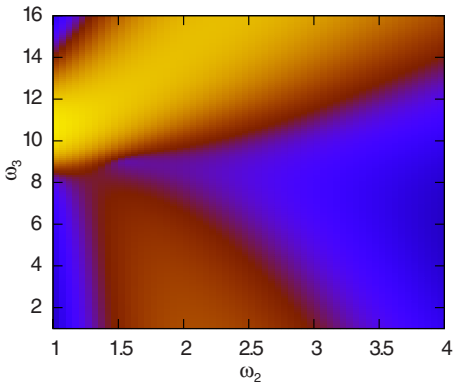

FIG. 17. (Color online) Density plot of the logarithm of the largest eigenvalue λ_{max} of the matrix of second derivatives of the free energy with respect to ω_2 and ω_3 at length $n=128$ (the lighter the shade, the larger the value).

ferent collapsed states. Such a transition has been seen to occur in the low-temperature behavior of the ISAW when a stiffness energy is added to model semiflexible polymers. One of the two low-temperature phases in that model is an ordered crystallinelike phase. Relatedly this occurs when the collapse is a first-order transition.

To test the possibility that the low temperature collapsed phase when $k>k_G$ is frozen we have plotted in Fig. 18 the proportion of steps of the trail *not* involved with a triply visited site. Given the collapsed nature of the phase it is appropriate to assume that the polymer has a surface [26] and so we plot our estimate against $1/n^{1/2}$. We have chosen a point in the $k=6$ model. The quantity $[1-3u_3(n)]$ is tending to zero as n is increased, suggesting that, proportionally, all sites of the trail will be triply visited: we can deduce that configurations produced are maximally dense and solidlike. In Fig. 19 we display a typical configuration produced by our simulations when $(\omega_2,\omega_3)=(1,10)$: it is space filling, forming a crystal-like structure, being almost totally made up of triply visited sites. We find the same behavior for the $k=k_G$ model at low temperatures.

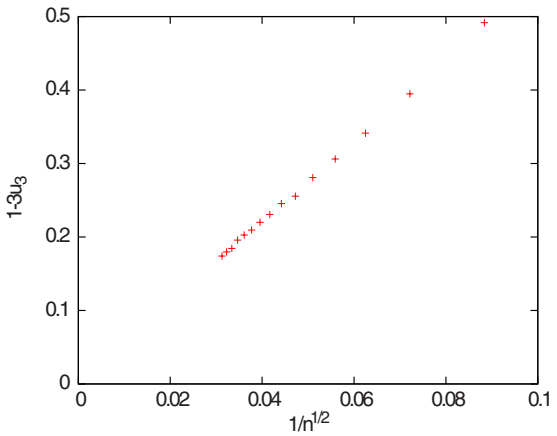

FIG. 18. (Color online) Plot of $1-3u_3(n)$, which measures the proportion of steps that are not involved with triply visited sites per unit length, against $1/\sqrt{n}$ at a point (1.58, 15.6) in the hypothesized frozen (crystal-like) phase. As the length increases this quantity vanishes.

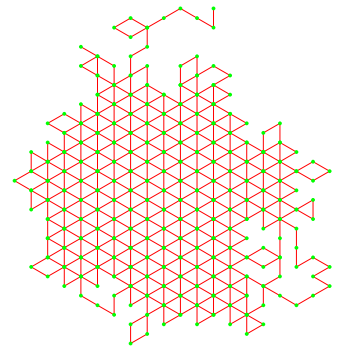

FIG. 19. (Color online) A typical configuration at length 512 produced at $(\omega_2,\omega_3)=(1,10)$ which looks like an ordered crystal.

For the sake of comparison we have considered the same quantity $1-3u_3(n)$ in the low-temperature region of the $k=2$ model. In Fig. 20 we plot the proportion of steps that are not involved with triply visited sites per unit length against $1/n^{1/2}$ at the point $(\omega_2,\omega_3)=(4,16)$: this quantity clearly converges to a nonzero value. In Fig. 21 we display a typical configuration produced by our simulations when $(\omega_2,\omega_3)=(5,1)$: while dense, the configuration still has internal holes and seems disordered. From the above considerations it seems that the phases that exist in our eISAT model on the triangular lattice are of a similar type to those in the semiflexible ISAW phase diagram [8–10], namely, a high-temperature swollen phase and two low-temperature phases: one is a disordered liquid-drop-like globular phase and the other is crystallinelike phase.

V. CONCLUSIONS

We can now build a complete picture of the phase diagram of the extended ISAT model on the triangular lattice. A schematic of the conjectured phase diagram is shown in Fig. 22. For small ω_2 and ω_3 we see the usual swollen polymer phase where $\nu=3/4$. For large enough ω_2 regardless of ω_3

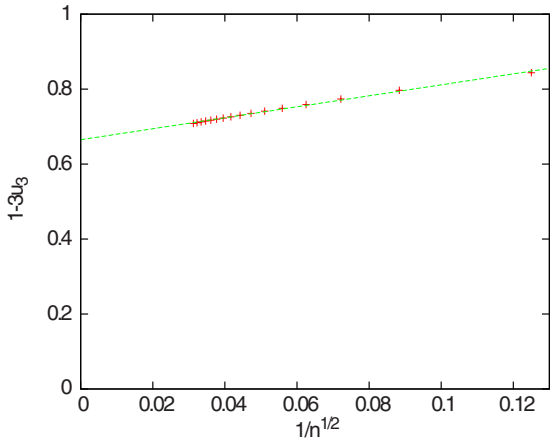

FIG. 20. (Color online) Plot of $1-3u_3(n)$, which measures the proportion of steps that are not involved with triply visited sites per unit length, against $1/\sqrt{n}$ at a point $(\omega_2,\omega_3)=(4,16)$ in the collapsed liquid-drop-like globule phase. As the length increases this reaches a nonzero value.

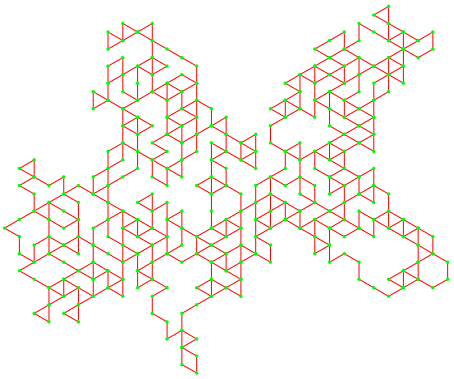

FIG. 21. (Color online) A typical configuration at length 512 produced at $(\omega_2,\omega_3)=(5,1)$, which is in the globule phase: it looks disordered and rather more like a liquidlike globule than a crystal.

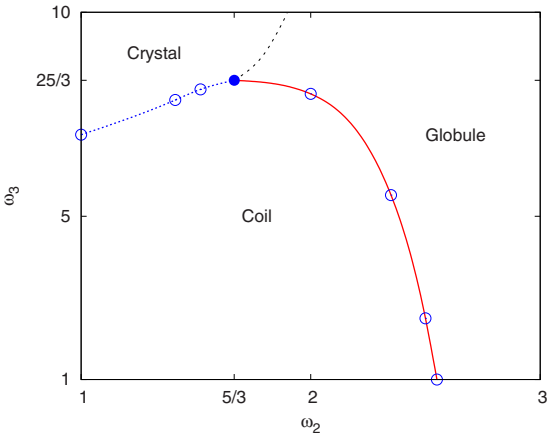

FIG. 22. (Color online) Schematic of the proposed phase diagram of the extended ISAT model on the triangular lattice. The filled circle is at the location of the kinetic growth point, and the open circles represent estimates of the collapse transition for various values of k. The dotted blue line is a line of first-order phase transitions, the full red line is a line of θ-point-like critical phase transitions, while the dashed gray line is also expected to be a line of critical phase transitions. We expect the two critical lines to be tangential as they approach the kinetic growth point.

we find a collapse phase as occurs in the ISAW model and a transition between the swollen and collapsed globule phases which seems to be θ-like. On the other hand for large enough ω_3 we find crystal-like configurations that are space filling and internally contain only triply visited sites. Between the swollen phase and the crystal-like phase the collapse transition is first order. Separating this line of first-order transitions from the line of θ-like transitions is a multicritical point: we have assumed that it is multicritical as its criticality is different to the two lines of critical points that connect to it. This point is precisely the point to which the kinetic growth process of trails maps.

It would seem that this larger parameter space has exposed a way of understanding the apparent differences and similarities of the ISAT and ISAW models. When ISAW is generalized with the addition of stiffness, and ISAT on a large enough coordination number lattice is generalized with different weightings for different numbers of visits, both display three polymer phases: swollen coil, globule, and polymer crystal. Note that for the eISAT model considered here, the crystal-like phase has nonzero entropy and as such is strictly speaking not a proper crystalline phase, but rather a maximally dense phase. This is in contrast to the polymer crystal phase found in the semiflexible ISAW model [8–10], where one finds zero-entropy β-sheet-like structures.

In two dimensions both semiflexible ISAW and eISAT have a first-order collapse transition between swollen coil and crystal-like phases, and a θ-point-like transition between swollen coil and globule phases. It is also apparent that the square lattice ISAT model is unusual in that it only displays the multicritical point, which is found in these generalized models as part of a larger phase diagram. It is not clear why the square lattice ISAT model displays the multicritical point rather than either the θ-like transition or the first-order transition.

ACKNOWLEDGMENTS

Financial support from the Australian Research Council via its support for the Centre of Excellence for Mathematics and Statistics of Complex Systems is gratefully acknowledged by the authors. J.D. was in part supported by the Japan Society for the Promotion of Science (JSPS) under Grant No. P09749. The FLATPERM simulations were performed on the computational resources of the Victorian Partnership for Advanced Computing (VPAC). A.L.O. thanks the School of Mathematical Sciences, Queen Mary University of London for hospitality.

[1] P.-G. de Gennes, *Scaling Concepts in Polymer Physics* (Cornell University Press, Ithaca, NY, 1979).
[2] J. des Cloizeaux and G. Jannink, *Polymers in Solution* (Clarendon Press, Oxford, 1990).
[3] P.-G. de Gennes, J. Phys. (France) Lett. **36**, L55 (1975).
[4] M. J. Stephen, Phys. Lett. A **53**, 363 (1975).
[5] B. Duplantier, J. Phys. (Paris) **43**, 991 (1982).
[6] B. Duplantier, EPL **1**, 491 (1986).
[7] B. Duplantier, J. Chem. Phys. **86**, 4233 (1987).
[8] U. Bastolla and P. Grassberger, J. Stat. Phys. **89**, 1061 (1997).
[9] J. Krawczyk, A. L. Owczarek, and T. Prellberg, Physica A **388**, 104 (2009).
[10] J. Krawczyk, A. Owczarek, and T. Prellberg, Physica A **389**, 1619 (2010).
[11] H. Noguchi and K. Yoshikawa, J. Chem. Phys. **109**, 5070 (1998).
[12] Y. Shapir and Y. Oono, J. Phys. A **17**, L39 (1984).
[13] H. A. Lim, A. Guha, and Y. Shapir, J. Phys. A **21**, 773 (1988).

[14] A. L. Owczarek and T. Prellberg, J. Stat. Phys. **79**, 951 (1995).
[15] T. Prellberg and A. L. Owczarek, Phys. Rev. E **51**, 2142 (1995).
[16] A. L. Owczarek and T. Prellberg, Physica A **373**, 433 (2007).
[17] P. Grassberger and R. Hegger, J. Phys. A **29**, 279 (1996).
[18] D. P. Foster, J. Phys. A: Math. Theor. **42**, 372002 (2009).
[19] B. Nienhuis, Phys. Rev. Lett. **49**, 1062 (1982).
[20] R. Brak, A. L. Owczarek, and T. Prellberg, J. Phys. A **26**, 4565 (1993).
[21] B. Duplantier and H. Saleur, Phys. Rev. Lett. **59**, 539 (1987).
[22] T. Prellberg and A. L. Owczarek, J. Phys. A **27**, 1811 (1994).
[23] H. Meirovitch, I. S. Chang, and Y. Shapir, Phys. Rev. A **40**, 2879 (1989).
[24] R. M. Bradley, Phys. Rev. A **41**, 914 (1990).
[25] T. Prellberg and J. Krawczyk, Phys. Rev. Lett. **92**, 120602 (2004).
[26] A. L. Owczarek, T. Prellberg, and R. Brak, Phys. Rev. Lett. **70**, 951 (1993).